Available online at www.sciencedirect.com
SCIENCE DIRECT®
ELSEVIER
Applied Energy 78 (2004) 137–149
APPLIED ENERGY
www.elsevier.com/locate/apenergy

Numerical analysis of heat transfer in a composite wall solar-collector system with a porous absorber

Wei Chen, Wei Liu*

School of Energy and Power Engineering, Huazhong University of Science and Technology, Wuhan, 430074, PR China

Received 18 June 2003; received in revised form 21 July 2003; accepted 26 July 2003

Abstract

In this paper, heat transfer and air flow in a composite-wall solar-collector system with a porous absorber has been studied. The 'unsteady' numerical simulation is conducted to analyze the performance of heat transfer and air flow in the composite wall. The excess heat is stored in the porous absorber by the incident solar radiation, which leads to a temperature gradient in the porous layer, so that the absorber can work as a good thermal-insulator when sunlight is not available. The influences of the particle size and the porosity of the porous absorber on the air temperature in the heated room are significant. The results show that all these factors should be taken into account for a better design of the passive solar-heating system.

1. Introduction

Passive solar-heating is often applicable in cold climates. The thermal storage wall has been used more extensively since the work of Trombe [1,2] was published. The standard Trombe wall has the drawback of low thermal resistance, which leads to heat losses at night or on cloudy days. Furthermore, as the heat storage and supply cannot be controlled, there is a possibility of overheating in the heated room. The application of a solar composite-wall may overcome this drawback. A composite

* Corresponding author. Tel.: +86-27-8754-2618.
E-mail addresses: weichen96@sina.com (W. Chen), w_liu@nxu.edu.cn (W. Liu).

0306-2619/$ - see front matter © 2004 Elsevier Ltd. All rights reserved.
doi:10.1016/j.apenergy.2003.07.003

Nomenclature

A_p	surface area of the porous absorber, m^2
A_{wi}	inside surface area of the thermal storage wall, m^2
A_{wo}	outside surface area of the thermal storage wall, m^2
c	specific heat, $J/(kg/K)$
C	inertia coefficient, defined in Eq. (10)
d	diameter, m
d_p	particle diameter of the porous layer, m
g	gravitational acceleration, m/s^2
G_{sun}	solar flux incident upon the glass cover, W/m^2
h_{wi}	convection heat-transfer coefficient between the air in the heated room and the inside surface of thermal storage wall, W/(mK)
k_f	fluid thermal conductivity, W/(mK)
k_m	apparent thermal conductivity, W/(mK)
k_s	thermal conductivity of solid phase of porous absorber, W/(mK)
k_w	thermal conductivity of thermal storage wall, W/(mK)
K	permeability of porous absorber, m^2
L_{po}	horizontal coordinate at the outside surface of porous absorber, m
L_{pi}	horizontal coordinate at the inside surface of porous absorber, m
P	pressure, Pa
Q_{ai}	convective heat exchange between the air inside the gap and the glass cover, J
Q_{ao}	convective heat exchange between the ambient and the glass cover, J
Q_{apo}	convective heat exchange between the air in the gap and the outside surface of porous absorber, J
Q_{api}	convective heat exchange between the air in the flow channel and the inside surface of porous absorber, J
Q_{aw}	convective heat exchange between the air in the flow channel and the outside surface of thermal storage wall, J
Q_{gp}	thermal radiation exchange between the glass cover and the outside surface of porous absorber, J
Q_{gsky}	thermal radiation exchange between the glass cover and the sky, J
Q_{inr}	heat flux from the composite wall to the heated room through the top vent, J
Q_{outr}	heat flux from the heated room to the composite wall through the bottom vent, J
Q_{pw}	thermal radiation exchange between the inside surface of the porous absorber and the outside surface of the thermal storage wall, J
T	temperature, K
T_{ao}	ambient temperature, K
T_p	temperature of the porous absorber, K
T_{room}	air temperature of the heated room, K
T_{wall}	temperature of the thermal storage massive wall, K

T_{walli}	temperature of the inside surface of thermal storage massive wall, K
u	velocity component in x-direction, m/s
$\lvert\vec{v}_d\rvert$	mean velocity($=\sqrt{u_d^2+v_d^2}$), m/s
v	velocity component in y-direction, m/s
V	volume, m^3
x	horizontal coordinate, m
y	vertical coordinate, m

Greek symbols

β	thermal expansion coefficient, 1/K
δ	transmissivity of the glass cover
τ	time, s
η_g	absorptivity of the glass cover
η_p	absorptivity of the outside surface of porous absorber
μ	dynamic viscosity, kg/(ms)
ρ	density, kg/m^3
θ	porosity of the porous medium, %

Subscripts

c	cold wall
d	Darcy
eff	effective
f	fluid
g	glass
m	apparent mean
p	porous
s	solid for porous absorber

wall solar collector system was studied [3], which consists of glazing, a massive wall and an insulating wall. There is a convective channel between the massive wall and the insulating wall, and no convective channel between the glazing and the massive wall. Another composite-wall solar-collector system with a porous absorber was also studied, in which a porous layer with vents is used between the glazing and the massive wall, or a non-convective porous layer, directly contacted to the massive wall, is conceived [4,5].

In the present study, a new kind of composite wall with a convective porous absorber shown schematically in Fig. 1 has been investigated. The numerical simulation was carried out to analyze the variation of flow and temperature fields in the composite wall and the effect of particle size and porosity of the porous layer on the

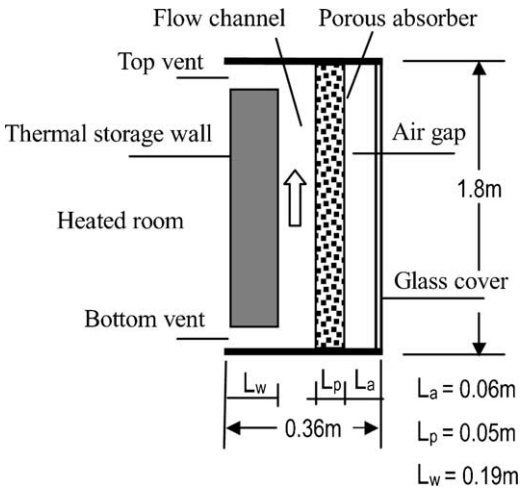

Fig. 1. Schematic of a composite wall solar collector with a porous absorber.

temperature of the heated room. The present study also focuses on the strategies for designing the composite wall in a passive solar building.

2. System description and mathematical analysis

2.1. System description

A composite-wall solar-collector system with a porous absorber is shown in Fig. 1. The composite wall, located on the south side of a heated room, consists of a glass cover, a massive thermal storage wall and a convective porous-layer that is located between the glass cover and the massive thermal storage wall. The porous layer is heated by the incident solar-radiation, through which the heat transfers to the air in the heated room and the massive thermal storage wall. The massive thermal storage wall has a top vent and a bottom vent to facilitate heat convection between the air inside the composite wall and the air in the heated room.

2.2. Theoretical modelling

The flow is assumed to be laminar and two-dimensional. The Boussinesq's approximation is applied to account for the air density variation. The flow in the composite wall (except the convective porous layer) is governed by the Navier–Stokes equation. The Brinkman–Forchheimer Extended Darcy model [6] is used to describe the flow in the convective porous-layer. The mathematical model is expressed below.

For flow and heat transfer in the composite wall (except the convective porous layer), the governing equations can be written as:

Continuity equation

$$\frac{\partial(\rho u)}{\partial x}+\frac{\partial(\rho v)}{\partial y}=0 \tag{1}$$

Momentum equations

$$\frac{\partial(\rho u)}{\partial \tau}+\frac{\partial(\rho u u)}{\partial x}+\frac{\partial(\rho v u)}{\partial y}=-\frac{\partial p}{\partial x}+\frac{\partial}{\partial x}\left(\mu\frac{\partial u}{\partial x}\right)+\frac{\partial}{\partial y}\left(\mu\frac{\partial u}{\partial y}\right) \tag{2}$$

$$\frac{\partial(\rho v)}{\partial \tau}+\frac{\partial(\rho u v)}{\partial x}+\frac{\partial(\rho v v)}{\partial y}=-\frac{\partial p}{\partial y}+\frac{\partial}{\partial x}\left(\mu\frac{\partial v}{\partial x}\right)+\frac{\partial}{\partial y}\left(\mu\frac{\partial v}{\partial y}\right)+\rho g\beta(T-T_C) \tag{3}$$

Energy equation

$$\rho c\frac{\partial T}{\partial \tau}+\rho c\left(u\frac{\partial T}{\partial x}+v\frac{\partial T}{\partial y}\right)=\frac{\partial}{\partial x}\left(k\frac{\partial T}{\partial x}\right)+\frac{\partial}{\partial y}\left(k\frac{\partial T}{\partial y}\right) \tag{4}$$

For flow and heat transfer in the convective porous layer, the governing equations can be written as:

Continuity equation

$$\frac{\partial(\rho u_{\mathrm{d}})}{\partial x}+\frac{\partial(\rho v_{\mathrm{d}})}{\partial y}=0 \tag{5}$$

Momentum equations

$$\frac{\rho}{\theta}\frac{\partial u_{\mathrm{d}}}{\partial \tau}+\frac{\rho}{\theta}\left(u_{\mathrm{d}}\frac{\partial u_{\mathrm{d}}}{\partial x}+v_{\mathrm{d}}\frac{\partial u_{\mathrm{d}}}{\partial y}\right)=-\frac{\partial p}{\partial x}+\frac{\partial}{\partial x}\left(\mu_{\mathrm{eff}}\frac{\partial u_{\mathrm{d}}}{\partial x}\right)+\frac{\partial}{\partial y}\left(\mu_{\mathrm{eff}}\frac{\partial u_{\mathrm{d}}}{\partial y}\right)-\frac{\mu u_{\mathrm{d}}}{K}+\frac{\rho C\theta}{\sqrt{K}}\left|\vec{v}_{\mathrm{d}}\right|u_{\mathrm{d}} \tag{6}$$

$$\frac{\rho}{\theta}\frac{\partial v_{\mathrm{d}}}{\partial \tau}+\frac{\rho}{\theta}\left(u_{\mathrm{d}}\frac{\partial v_{\mathrm{d}}}{\partial x}+v_{\mathrm{d}}\frac{\partial v_{\mathrm{d}}}{\partial y}\right)=-\frac{\partial p}{\partial y}+\frac{\partial}{\partial x}\left(\mu_{\mathrm{eff}}\frac{\partial v_{\mathrm{d}}}{\partial x}\right)+\frac{\partial}{\partial y}\left(\mu_{\mathrm{eff}}\frac{\partial v_{\mathrm{d}}}{\partial y}\right)-\frac{\mu v_{\mathrm{d}}}{K}+\frac{\rho C\theta}{\sqrt{K}}\left|\vec{v}_{\mathrm{d}}\right|v_{\mathrm{d}}+\rho g\beta(T-T_{\mathrm{c}}) \tag{7}$$

Energy equation

$$(\rho c)_{\mathrm{m}}\frac{\partial T}{\partial \tau}+\rho c\left(u_{\mathrm{d}}\frac{\partial T}{\partial x}+v_{\mathrm{d}}\frac{\partial T}{\partial y}\right)=\frac{\partial}{\partial x}\left(k_{\mathrm{eff}}\frac{\partial T}{\partial x}\right)+\frac{\partial}{\partial y}\left(k_{\mathrm{eff}}\frac{\partial T}{\partial y}\right) \tag{8}$$

In the above set of equations, all variables, coefficients and constants are defined in the nomenclature. Eqs. (5)–(8) are used to model heat convection in the porous

absorber. Eqs. (6)–(7) contain the general terms of viscosity force and pressure gradient known as Darcy's law, which is extended by the further inclusion of terms modeling advective inertia, boundary effects (Brinkman term) and form-drag (Forchheimer inertia). Eq. (7) contains an additional buoyancy term. The values of permeability K and inertia coefficient C in the momentum equations are estimated for the packed porous bed with rock diameter d_r and porosity θ [7,8].

$$K = \frac{d_r^2 \theta^3}{175(1-\theta)^2} \tag{9}$$

$$C = \frac{1.75}{\sqrt{175}} \theta^{-3/2} \tag{10}$$

Physical properties of the porous materials are needed in the calculation. It has been found that taking $\mu_{eff} = \mu_f$ in Brinkman's extension provides a good agreement with the experimental data [9] and is adopted in the present work. In addition, k_m and $(\rho c)_m$ are calculated by $k_m = \theta k_f + (1-\theta)k_s$ and $(\rho c)_m = \theta(\rho c)_f + (1-\theta)(\rho c)_s$ [10].

2.3. Boundary and initial conditions

Numerical simulations were performed under the ambient and operative conditions. A typical cold and sunny day of November in Wuhan, China was considered, and the outdoor temperature [11] and the solar radiative variation [12] were given by Eqs. (11) and (12).

$$T_{ao}(\tau) = \overline{T_{ao}} + T_{ar}\cos\left(\frac{\pi}{12}(\tau - 14)\right) \tag{11}$$

$$G_{sun}(\tau) = \hat{G}_{sun}\sin\left(\frac{\tau - a}{b - a}\pi\right) a < \tau < b \tag{12}$$

where $\overline{T_{ao}}$ is for an average outside temperature of 10 °C; T_{ar} for amplitude temperature of 5 °C; $\hat{G}_{sun}$ for maximum solar radiation of 350 W/m^2; a for sunrise hour at 6:00 o'clock in the morning; b for sunset hour at 18:00 o'clock in the afternoon; τ for time hours. The assumptions for the energy equilibrium equations of the composite wall with a porous absorber have been considered as follows.

1. A uniform temperature for the air in the composite wall is considered.
2. No temperature gradient exists on the surfaces of the glass cover, porous absorber and thermal storage wall in the composite wall.
3. All surfaces of the glass cover, porous layer and thermal storage wall in the composite wall are considered as grey bodies.
4. The walls of the solar system except the south thermal storage wall of the heated room, the bottom and the roof of the heated room and the upper and bottom ends of the composite wall are considered as thermal insulators.

The fluid in the composite wall solar system is initially stagnant and at a uniform temperature which is the same as the ambient temperature. The inlet velocity of airflow into the composite wall has been estimated by the velocity magnitude of internal flow. The boundary conditions from the energy equilibrium equations are given below.

For the inside surface of the glass cover:

$$\eta_g G_{sun} + Q_{gsky} + Q_{gp} + Q_{ai} + Q_{ao} = 0, \quad T = T_g, u = 0, v = 0 \tag{13}$$

For the outside surface of porous absorber:

$$x = L_{po}, \ k_m A_p \frac{dT_p}{dx} = \delta\eta_p G_{sun} A_p + Q_{gp} + Q_{apo}, \ u\Big|_{y=L_{po}^-} = u\Big|_{y=L_{po}^+}, v\Big|_{y=L_{po}^-} = v\Big|_{y=L_{po}^+}, p\Big|_{x=L_{po}^-} = p\Big|_{z=L_{po}^+}, \mu_m\left(\frac{\partial u_d}{\partial y} + \frac{\partial v_d}{\partial x}\right)\Big|_{x=L_{po}^-} = \mu\left(\frac{\partial u}{\partial y} + \frac{\partial v}{\partial x}\right)\Big|_{x=L_{po}^+} \tag{14}$$

For the inside surface of porous absorber:

$$x = L_{pi}, \ k_m A_p \frac{dT_p}{dx} = Q_{pw} + Q_{api}, u\Big|_{y=L_{pi}^-} = u\Big|_{y=L_{pi}^+}, v\Big|_{y=L_{pi}^-} = v\Big|_{y=L_{pi}^+}, p\Big|_{x=L_{pi}^-} = p\Big|_{z=L_{pi}^+}, \mu_m\left(\frac{\partial u_d}{\partial y} + \frac{\partial v_d}{\partial x}\right)\Big|_{x=L_{pi}^-} = \mu\left(\frac{\partial u}{\partial y} + \frac{\partial v}{\partial x}\right)\Big|_{x=L_{pi}^+} \tag{15}$$

For the outside surface of thermal storage wall:

$$k_w A_{wo} \frac{\partial T_{wall}}{\partial x} = Q_{pw} + Q_{awi}, \ u = 0, v = 0 \tag{16}$$

For the inside surface of thermal storage wall:

$$k_w \frac{\partial T_{wall}}{\partial x} = h_{wi}(T_{room} - T_{wall}), \ u = 0, v = 0 \tag{17}$$

For the air in the heated room:

$$(\rho c)V \frac{\partial T_{room}}{\partial \tau} = Q_{inr} + Q_{outr} + h_{wi} A_{wi}(T_{wall} - T_{room}) \tag{18}$$

3. Numerical procedure

For the present study, the governing Eqs. (1)–(4) and (5)–(8) together with the boundary conditions mentioned above were solved with the SIMPLER method [13], which is validated for various cases [14]. The computer code is based on the mathematical formulation discussed earlier. The control–volume formulation utilized in this method ensures continuity of convective and diffusive fluxes as well as momentum and energy conservations. This method allows the numerical treatment of pure conduction in the solid of the massive thermal storage wall by introducing an artificial viscosity,

which ensures that a zero velocity prevails throughout the calculated region. The harmonic mean formulation was used to handle abrupt variations in thermal physical properties, such as permeability and thermal conductivity, across the interface, for example, at the porous/fluid layer interface. This can ensure the continuity of convective and diffusive fluxes across the interface without requiring the use of an excessively fine grid-structure.

Non-uniform mesh sizes were used for the numerical computation. The grid in the horizontal direction was uniformly distributed. In the vertical direction, finer mesh sizes were taken within the porous absorber. To test the grid independence, two different grid sizes, 128×88 and 128×108, had been employed in the present study, but its influence on the calculating results is small. Therefore, a grid of 128×88 was chosen.

As to the unsteady-state numerical calculations, the time step $\Delta\tau$ was of much concern and several values of $\Delta\tau$ were examined. For example, it had been found that the maximum deviation between the calculated results by using $\Delta\tau=30$ s and $\Delta\tau=45$ s was only 2%. Hence, the time step of $\Delta\tau=45$ s together with the grid size of 128×88 were used for the unsteady-state numerical calculations performed in this study.

The porous layer, made of quartzite, and the thermal storage wall, made of concrete, were chosen in the simulation with the following physical properties [15].

Quartzite: $\rho = 2635\ \text{kg/m}^3$, $c = 0.732\ \text{kJ/(kgK)}$, $k_\text{p} = 5.17\ \text{W/(mK)}$

Concrete: $\rho = 2243\ \text{kg/m}^3$, $c = 0.837\ \text{kJ/(kgK)}$, $k_\text{s} = 1.173\ \text{W/(mK)}$

The volume of the selected heated room is 16.2 m^3, in which the air is heated by the composite-wall solar-collector.

4. Results and discussion

The effects of the porous absorber on the temperature distribution and airflow in the composite wall have been analyzed. To discuss the influences of particle size and porosity of the porous absorber on the temperature of heated room, we made a numerical calculation for the present model. The results are analyzed as follows.

Observing Fig. 2, we can find that, during the heating period, the surface of the porous absorber has a comparatively higher temperature: thus the solar radiation absorbed by the porous layer is utilized to raise the air temperature and the thermal storage wall temperature. When solar radiation is not available, as the heat has already been stored in the massive thermal storage wall, this wall with a relatively higher temperature can still heat the air in the room.

Convective heat transfers occur in the flow channel, the gap and the porous absorber, so the air is heated in the composite wall. As shown in Fig. 3, inside the composite wall, the air temperature near the bottom vent is relatively lower, but the air temperature near the top vent is higher. From the bottom to the top inside the composite wall, the temperature rises gradually. The heated air goes through the top

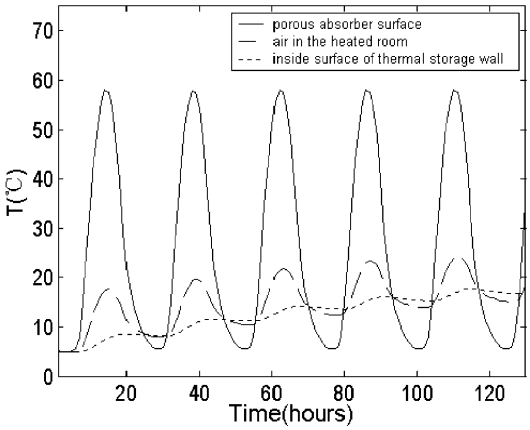

Fig. 2. Comparison among predicted values of temperature for a porous absorber surface, air in the heated room and inside surface of thermal storage wall.

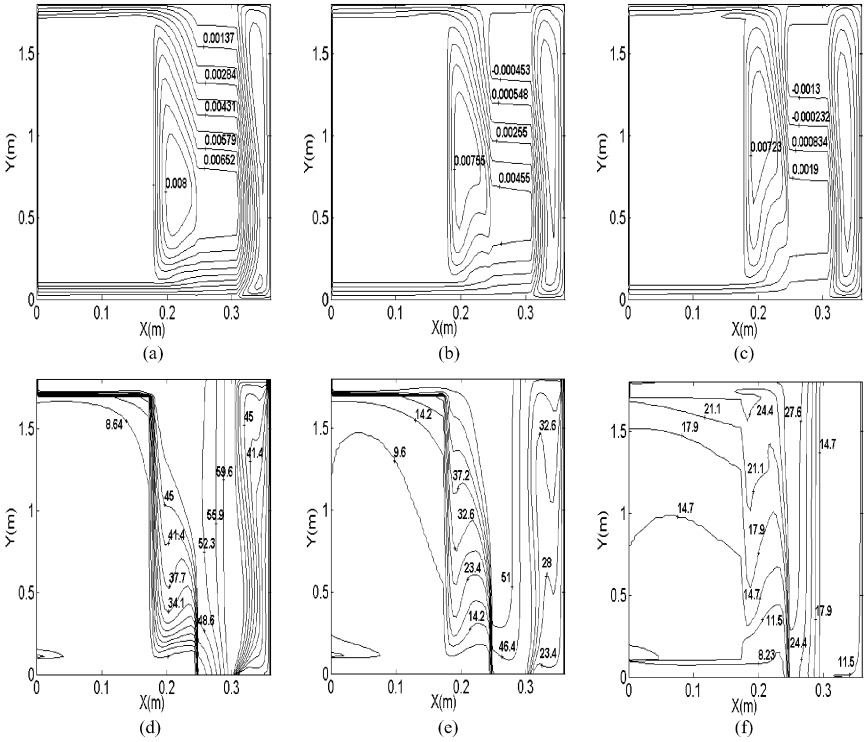

Fig. 3. Development of flow and temperature fields with time for the composite wall with porous absorber (particle diameter 1 cm and porosity of porous absorber 0.25): (a) streamlines at 12:00 noon; (b) streamlines at 16:00 in the afternoon; (c) streamlines at 19:00 in the evening; (d) isotherms (°C) at 12:00 noon; (e) isotherms (°C) at 16:00 in the afternoon; (f) isotherms (°C) at 19:00 in the evening.

vent into the heated room, while the room air is drawn through the bottom vent into the composite wall to be heated, which forms an air cycle in the heating system. The comparison of flow and temperature fields inside the solar composite wall at 12:00 noon, 16:00 in the afternoon and 19:00 in the evening can show that the peak temperature moves with time from the outside surface to the inside of the porous absorber. When the sun is shining at 12:00 noon and at 16:00 in the afternoon, convective heat-transfers in the flow channel, the air gap and the porous absorber are intensified. In contrast, when no solar radiation is available at 19:00 in the evening, the air convection is then strongly reduced and the temperature of the outside surface of the porous absorber is much lower than that of the inside surface of porous absorber. Thus the convective and the radiative heat-exchanges between the composite wall and the ambient decrease, and the heat loses of the system is greatly reduced. As the excess heat is stored in the porous thermal storage absorber by incident solar radiation and there is a great temperature gradient in this layer, the temperature of the inside surface of absorber is comparatively higher. Therefore, when the sun is not shining, the porous layer can serve as a semi-thermal insulator.

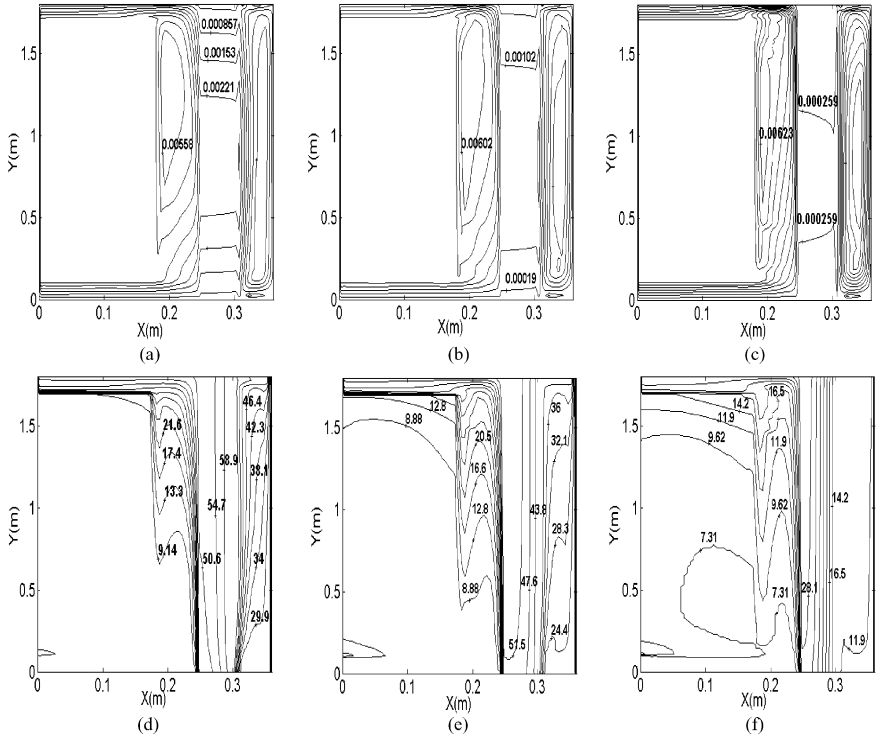

Fig. 4. Development of flow and temperature fields with time for composite wall with porous absorber (particle diameter 1 cm and porosity of porous absorber 0.1): (a) streamlines at 12:00 noon; (b) streamlines at 16:00 in the afternoon; (c) streamlines at 19:00 in the evening; (d) isotherms (°C) at 12:00 noon; (e) isotherms (°C) at 16:00 in the afternoon; (f) isotherms (°C) at 19:00 in the evening.

Comparison between Figs. 3 and 4 can show that the effects of porosity of porous layer on the temperature distribution and the flow in the composite wall are significant. During the time of heating, such as at 12:00 noon and at 16:00 in the afternoon, the decrease in the porosity of the porous absorber from 0.25 to 0.1 for the same particle size results in the reduction in heat convection between the air in the gap and the air in the flow channel, which leads to an increase in the temperature difference, so that the heat gained by the thermal storage wall and the heated room reduces. When no sunlight is available, such as at 19:00 in the evening, the heat loss of the heating system decreases, and the temperature of the solar composite wall is relatively lower than that with incident solar radiation.

The variation of air temperature in the heated room with time at different particle sizes and porosity of the porous absorber is depicted in Fig. 5. It can be seen that the influences of particle size and porosity of the porous absorber on the air temperature in the heated room are significant. With an increase in particle size and porosity of the porous layer, there will be a possibility of overheating in the heated room. By contrast, with a decrease in particle size and porosity of the porous layer, solar energy cannot be fully used to meet the needs of heating. Therefore, the particle size and the porosity of porous absorber should be chosen properly.

In addition, for a better design of the passive-solar system, a suitable massive wall with better function of thermal storage should be considered with a top vent and a bottom vent allowing the air flow between the composite wall and the heated room, and dampers should be set both at the top vent and the bottom vent to open or block off the air circulation in the ventilated room. So unwanted solar energy supply in the summer is limited and the reverse heat circulation is also forbidden in the operation.

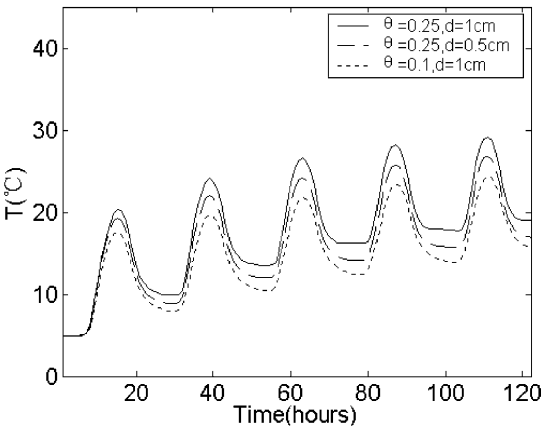

Fig. 5. Comparison among predicted values of temperature for the heated room versus different diameters and porosities of porous absorber.

5. Conclusions

A numerical model has been developed to study the effects of the porous absorber on the temperature distribution and the airflow in the composite wall solar collector system. We have found that the possibility of overheating in the heating system decreases greatly and the thermal resistance of the composite wall increases at night or on a cloudy day, if a convective porous layer is used as a solar absorber inside the composite wall. As some excess heat is stored by incident solar radiation and a temperature gradient exists in the porous absorber, this layer can work as a semi-thermal insulator when solar radiation is not available. The influences of particle size and porosity of the porous absorber on the air temperature in the heated room are significant, which should be considered to avoid the occurrence of overheating and ineffective use of solar energy. Therefore, in a passive-solar heated building, the composite wall with a porous absorber under investigation can work better in saving energy than the Trombe wall in winter, if the particle size and the porosity of the porous absorber are chosen properly.

Acknowledgements

The current work is financially supported by National Key Basic Research Development Program of China (No. G2000026303), National Natural Science Foundation of China and Doctoral Foundation of Education Ministry of China (No. 2000048731).

References

[1] Trombe F. Maisons solaires. Techniques de l'IngTenieur 1974; 3:C777.
[2] Ben Yedder R, Bilgen E. Natural convection and conduction in Trombe wall systems. International Journal of Heat and Mass Transfer 1991;34(4/5):1237.
[3] Zrikem Z, Bilgen E. Theoretical study of a composite Trombe–Michel wall solar collector system. Solar Energy 1987;39(5):409–29.
[4] Du Z-G, Bilgen E. Natural convection in composite-wall collectors with porous absorber. Solar Energy 1990;45(6):325–32.
[5] Mbaye M, Bilgen E. Natural convection and conduction in a porous wall: solar collector systems without vents. Journal of Solar Energy Engineering, Transactions of ASME 1992;114(2):40–6.
[6] Rees DAS. The onset of Dary–Brinkman convection in a porous layer: an asymptotic analysis. International Journal of Heat and Mass Transfer 2002;45:2213–20.
[7] Ergun X. Fluid flow through packed columns. Chemical Engineering Progress 1952;48:89–92.
[8] Beckermann C, Ramadhyani S, Viskanta R. Natural convection flow and heat transfer between a fluid layer and a porous layer inside a rectangular enclosure. J Heat Transfer 1987;109(5):363–70.
[9] Neale G, Nader W. Practical significance of Brinkman's extension of Darcy's law. Canadian Journal of Chemical Engineering 1974;53:475–8.
[10] Chen Falin, Chen CF. Convection in superposed fluid and porous layers. J Fluid Mech 1992;234:97–119.
[11] Shao-Zhong Kang. Computer simulation of water transport in soil–plant–atmosphere continuum. Shui Li Xue Bao 1992;3:1–12.

[12] Suning Zhang. The institution of the hourly solar-radiation model. Acta Energiae Solaris Sinica 1997;18(3):273–7.
[13] Patankar SV. Numerical heat transfer and fluid flow. New York: Hemisphere Publishing Corp; 1980.
[14] Wen-Quan Tao. Numerical heat transfer (2nd ed). Xi'an Jiaotong University Press; 2001.
[15] Qing-Fang Ma. Practical thermal physical property handbook. The Chinese Agriculture Mechanics Press; 1986.